

Supplementary Information

High Affinity scFv-hapten Pair as a Tool for Quantum Dot Labeling and Tracking of Single Proteins in Live Cells

Gopal Iyer^{1,*}, Xavier Michalet^{1,*}, Yun-Pei Chang¹, Fabien F. Pinaud^{1,§}, Stephanie E.

Matyas², Gregory Payne³, Shimon Weiss^{1,4,*}

¹Dept of Chemistry & Biochemistry, UCLA, Los Angeles, CA

² Hematology/Oncology, David Geffen School of Medicine, UCLA, Los Angeles, CA

³Dept of Biological Chemistry, David Geffen Medical School, UCLA, Los Angeles, CA

⁴Dept of Physiology, David Geffen Medical School, Los Angeles, CA

* Corresponding authors: gopal@chem.ucla.edu, michalet@chem.ucla.edu,
sweiss@chem.ucla.edu

§Present address: Dept of Biology, Ecole Normale Supérieure, Paris, France

Supplementary Methods

Chemicals, antibodies and peptides

Alexa Fluor 647 anti-myc antibody and fluorescein-dextran were purchased from Invitrogen (Carlsbad, CA). Crude peptides with sequence: FITC-GSESGGSESGFCCFCCFCCF-CONH₂ (FL-peptide or FL-P) and KGSESGGSESGFCCFCCFCCF-CONH₂ (K-peptide or K-P) were purchased from Anaspec (San Jose, CA). Polyethylene glycol reagents (PEG 330) were obtained from

Pierce Biotechnology (Rockford, IL). All chemicals used for QD solubilization were purchased from Sigma-Aldrich (St. Louis, MO).

Peptide coating, PEGylation and characterization of QDs

TOPO-coated CdSe/ZnS QDs were synthesized as described¹. CdSe cores (diameter: 4.7 nm) were coated with 4-5 monolayers of ZnS and preserved in butanol/trioctylphosphine (TOPO). The resulting red emitting QDs (emission peak: 620 nm) were solubilized in aqueous buffer by peptide exchange as described^{2,3}. Briefly, 20 µl of 1 µM TOPO-coated QDs was adjusted to 450 µl with pyridine. 4 mg of FL-p were added for 100% FL-p QD coating; for 50 % (resp. 10 %) FL-p QD coating, 2mg of FL-p and 2 mg of K-p (resp. 0.4 mg of FL-p and 3.6 mg of K-p) dissolved in 50 µl DMSO were added and mixed with addition of tetramethylammonium hydroxide 25%(w/v) in methanol. The resulting mixture was spun at 12,000 rpm for 3 min, the supernatant decanted and the remaining pc-QDs resuspended in 300 µl DMSO. 300 µl of pc-QDs were eluted from a Sephadex G-25 column (Amersham Biosciences, Sunnyvale, CA) equilibrated with milli-Q water, checking for the presence of QD by monitoring the red QD fluorescence using a hand held ultraviolet lamp emitting at 254 nm. Excess peptides from the pc-QD containing fractions were first dialyzed overnight against a solution of 50 mM borate, 10 mM Na-phosphate and then for 4-6 hr against a solution of 100 mM borate, 10 mM NaCl, pH 8.0 using a 300,000 MWCO PVDF dialysis membrane (Spectra/Por, SpectrumLabs, Rancho Dominguez, CA). QDs coated with a FL-p:K-p ratio of 50:50 and 100:0 were found to be stable for over a month at 4°C in PBS buffer (pH 7.2), whereas QDs coated with a FL-p:K-p ratio of 10:90 were stable of one week.

PEGylation of 50 % and 10 % FL-pc-QDs was carried out in the presence of 1 mM NHS-PEG330 for 1 hr in 100 mM NaH_2PO_4 , 100 mM NaCl, pH 7.4. Conjugation was terminated with 10 mM Tris-Cl, pH 6.8. Purified pc-QDs were electrophoresed at 120 V on a 1% TBE agarose gel. Gels were visualized using a fluorescence gel scanner (Molecular Imager FX Pro Plus, Biorad, Hercules, CA) equipped with a laser excitation source at 488 nm and appropriate emission filters.

Quantification of the number of FL molecules per FL-pc-QD

The principle of FL and QD quantification in a FL-pc-QD sample has been described in detail in ref. ³. We reproduce it here for completeness. Absorption curves used for this analysis are shown in Fig. 2.

A simple way to obtain the number of FL-p coating each QD is by light absorption measurement. Absorption of light at a wavelength λ by a FL-pc-QD can have several causes: (i) absorption by the QD if $\lambda < \lambda_{\text{QD}}$ (where λ_{QD} is the first exciton peak of QD absorption), (ii) absorption by FL if $\lambda < \lambda_{\text{FL}}$ (where λ_{FL} is the upper limit of the absorption of FL), and (iii) absorption by the peptides themselves. The latter is negligible at visible wavelengths, and therefore it is easy to obtain two very separate situations: (1) one in which only the QDs are absorbing ($\lambda_{\text{FL}} < \lambda < \lambda_{\text{QD}}$), and (2) the other where both FL and QDs are excited ($\lambda < \lambda_{\text{FL}} < \lambda_{\text{QD}}$).

Let n be the unknown average number of FL-p per QD. The extinction coefficient of FL at 493 nm, $\epsilon_{\text{FL}}(493)$, is provided by the manufacturer ($\epsilon_{\text{FL}}(493) = 85,200 \text{ cm}^{-1} \text{ M}^{-1}$). The first exciton peak of the QD used in this experiment is 610 nm.

If we measure the absorption of a FL-pc-QD at 493 nm and 610 nm, we will obtain data corresponding to the two different situations described above.

The total absorption at a wavelength λ will read:

$$A_{FL-pc-QD}(\lambda) = \left[\varepsilon_{QD}(\lambda) + n \cdot \varepsilon_{FL}(\lambda) \right] c_{QD} L, \quad (1)$$

where c_{QD} and L are the QD concentration and the excitation path length respectively.

The extinction coefficient of CdSe QDs (at their first exciton peak wavelength) has been experimentally measured by Peng and collaborators^{4,5} to depend on the first exciton peak wavelength according to:

$$\begin{aligned} \varepsilon_{QD} &= 5857D^{2.65} \\ D &= \left(1.6122 \cdot 10^{-9}\right)\lambda^4 - \left(2.6575 \cdot 10^{-6}\right)\lambda^3 + \left(1.6242 \cdot 10^{-3}\right)\lambda^2 - (0.4277)\lambda + (41.57) \end{aligned} \quad (2)$$

where D is the diameter of the quantum dot core in nm, and ε is expressed in $M^{-1}cm^{-1}$.

From Eq. (2), we can calculate $\varepsilon_{QD}(610)$, and by reporting it in Eq. (1) written for $\lambda = 610$ nm, obtain the QD concentration:

$$c_{QD} = \frac{A_{FL-pc-QD}(610)}{\varepsilon_{QD}(610)L}. \quad (3)$$

Writing Eq. (1) for $\lambda = 493$ nm, we obtain the following equation for n :

$$n = \frac{\left[\frac{A_{FL-pc-QD}(493)}{A_{FL-pc-QD}(610)} \varepsilon_{QD}(610) - \varepsilon_{QD}(493) \right]}{\varepsilon_{FL}(493)}. \quad (4)$$

The only unknown in this expression is $\varepsilon_{QD}(493)$, which can be easily obtained from $\varepsilon_{QD}(610)$ and the measurement of the QD-only absorption spectrum:

$$\varepsilon_{QD}(493) = \varepsilon_{QD}(610) \frac{A_{QD}(493)}{A_{QD}(610)} \quad (5)$$

The number of FL-p per QD is thus given by the following equation:

$$n = \left[\frac{A_{FL-pc-QD}(493)}{A_{FL-pc-QD}(610)} - \frac{A_{QD}(493)}{A_{QD}(610)} \right] \frac{\varepsilon_{QD}(610)}{\varepsilon_{FL}(493)}. \quad (6)$$

The number obtained for the 100:0 mixture ($n = 25$) was comparable to that obtained previously ($n = 20$) for a similar sample³.

Yeast surface display

Yeast strain EBY100 *MATa ura3-52 trp1 leu2Δ1 his3Δ200 pep4::HIS3 prb1Δ1.6R can1 GAL* (pIU211:*URA3*) harboring pCT-4M5.3⁶ (4M5.3 scFv) was grown in 5 ml media containing SDCAA (2 % dextrose, 0.67 % yeast nitrogen base, 0.5 % casamino acids, 50 mM sodium phosphate buffered to pH 6.6). Growth took place at 30 °C in a 250 rpm shaker for 24 hr until an OD₆₀₀ of 2 was reached. For induction, cells were first centrifuged and re-suspended in SGCAA (in which galactose replaces the dextrose in SDCAA) to an OD₆₀₀ of 0.5. Cells were then grown at 20 °C in a 250 rpm shaker for 24 - 36 hr.

Yeast labeling

Yeast cells in exponential phase at OD₆₀₀ 1 (2.10^6 cells/ml) were harvested by centrifugation, washed in ice cold 1X PBSF buffer (3.2 mM Na₂HPO₄, 0.5 mM KH₂PO₄, 1.3 mM KCl, 135 mM NaCl, pH 7.4, 0.1 % bovine serum albumin). All labeling steps were performed on ice and at 4 °C. For ensemble imaging (confocal and wide-field epifluorescence), 10 μM FL-dextran (MW = 2.10^6 , Invitrogen), 1:100 of mouse anti-myc-tag monoclonal antibody (Clone 9B11), Alexa Fluor 647 conjugated (Invitrogen), or 10 nM FL-pc-QDs were used. Incubation of antibodies, FL-pc-QDs or FL-dextran was carried out at 4 °C for 30 min. For FACS experiments, variable concentrations of FL-pc-QDs or FL-dextran were used and incubation times were extended to 3 hrs, as described⁶.

Cells were washed twice with ice cold PBSF before injection in the FACS reader. For single QD imaging, cells were incubated with 30 pM of FL-pc-QDs for 30 min.

Fluorescence-Aided Cell Sorting Analysis

Growth, induction, labeling and titration of FL-pc-QDs of 4M5.3 surface-displaying yeast were carried out as described previously⁷. 1 pM to 600 nM FL-pc-QDs with varying FL-p:K-p ratios were incubated with yeast cells for 30 min and analyzed by flow cytometry. Labeled yeast samples were measured using the BD FACSAria (Becton Dickinson, Franklin Lakes, NJ) digital cell sorter equipped with BD FACSDiVa software. The cytometer has three lasers emitting at 488, 633, and 405 nm. The 488 nm laser was used to excite FITC, whose emission was detected using a 530/30 filter. The 405 nm laser was used to excite QDs, whose emission was detected using a 610/20 filter. Yeast cells were gated based on their forward versus side scatter profile and fluorescence was measured in a 2-dimensional plot of FITC versus QD. A negative control was used to set the voltages for all parameters. Single-color control for FITC indicated that no compensation was necessary.

FACS data were imported and analyzed using software written in LabView (National Instruments, Austin, TX). The (arithmetic) mean fluorescence signal of the gated cells in each channel (FL or QD) was used to plot titration curves (Fig. 4 & S3). In particular, we made sure to reject cells with fluorescence signal < 0 (in either FL or QD channel), corresponding to cells with signal below background level. For the 10 % FL-pc-QD samples, the percentage of rejected cells according to this criterion was ~ 70 % throughout the whole concentration range (1 pM- 600 nM), while for the 50 % and 100 % FL-pc-QD samples, the percentage of rejected cells ranged from 10 to 80 % and from 40

to 80 % respectively, depending on the concentration as illustrated in Fig. S4. For these two samples, the percentage of cells retained for analysis could be fitted with the same simple binding model⁷ used for the fluorescence signal itself. The fitted K_D 's were comparable to the values obtained for the QD fluorescence signal. This behavior is expected, as low FL-pc-QD concentration result in low level of yeast cell labeling and therefore weak signal (below threshold). In particular, the FACS reader appeared to have poorer performance in terms of excitation and detection of the QD signal than for the FL signal, for reasons that we have not been able to determine. As a consequence, the QD signal never really goes much above the background level in the case of the 10 % FL-pc-QD sample, except at the highest concentrations. This phenomenon explains the late surge in QD signal shown on the upper right curve of Fig. S3 and the artificially high K_D^{QD} values fitted for this sample.

The dissociation constants K_D obtained from FACS measurements were similar for all samples, with an average value of 6.9 ± 5.1 nM (resp. 9.6 ± 3.8 nM) as measured from the FL signal (resp. QD signal) (Fig. 4). Interestingly, these values are 4-5 orders of magnitude larger than those reported for the interaction of free FL-biotin with free 4M5.3 scFv⁶. Since a similarly large K_D value was obtained for FL-dextran using the same method, we attribute this apparent discrepancy to the impaired ability of FL to bind to 4M5.3 scFv due to its reduced accessibility when displayed on the cell wall (Fig. 3B). Although the crowded environment of the QD's surface itself may play a role in this reduced binding efficiency, its effect is presumably smaller since the measured K_D s are similar to that obtained for FL-dextran. However, the different local environments of FL

in FL-pc-QDs covered with different amounts of FL-p and K-p could explain the small increase of K_{DS} (i.e. lower binding efficiency) at larger FL-coverage.

Mammalian cell line expression

The scFv 4M5.3 cDNA sequence was inserted between the signal peptide (aa 1-23) and the rest (aa 24-254) of the full length sequence of mouse prp with epitope 3F4. The chimeric scFv-Prp construct was cloned into cDNA3 (Invitrogen) and transfected into mouse neuroblastoma cell line N2a (ATCC) using transfectamine 2000 (Invitrogen) following the manufacturer's protocol. Stable clones were selected using 0.8 mg/ml G418. All cells were maintained in DMEM (Invitrogen) supplemented with 10 % fetal bovine serum.

Labeling of N2a cells

N2a cells and N2a cells transfected with scFv-Prp were grown on polylysine-coated coverslips to 50-80 % confluence. After one wash with Hank's buffer salt solution (HBSS, Invitrogen), cells were blocked by 1 % bovine serum albumin (BSA) in HBSS for 1 hr at 37 °C. For labeling, cells were then incubated with FL-pc-QDs with 1% BSA in HBSS for 10 min at RT before extensive wash with HBSS buffer. For ensemble confocal microscopy, 2-10 nM FL-pc-QDs were used. For single-molecule tracking experiments, 1-10 pM FL-pc-QDs were used.

Fluorescence microscopy

Wide-field epifluorescence microscopy of yeast cells was performed on an inverted microscope (Axiovert 100, Zeiss, Thornwood, NY) equipped with a 100 W Mercury lamp, an oil immersion objective (x 63, NA 1.4, Zeiss) and appropriate combination of filters and dichroic mirrors. Images were acquired with a CCD camera (CoolSnap HQ,

Photometrics, Tucson, AZ) controlled by Metamorph (Molecular Devices, Sunnyvale, CA). Confocal microscopy of yeast cells was performed using a custom-made stage-scanning confocal microscope similar to that described in ref.⁸. In some experiments, this system was replaced by a spinning-disk confocal microscope (CSU-10, Yokogawa, Japan, data not shown). Live cells were immobilized between a glass coverslip and an agarose cushion. Total internal reflection fluorescence (TIRF) microscopy of N2a cells was performed on a custom-modified inverted microscope (IX71, Olympus, Center Valley, PA) equipped with a back-illuminated EMCCD camera (Cascade 512B, Photometrics). The 488 nm line of an argon-ion laser was used for excitation (2-6 mW average power) and a 625DF25 emission filter used for detection. Movies of 1,000 frames (100 ms/frame) were acquired using WinView (Photometrics). Single-molecule trajectories were reconstructed and analyzed as described⁹.

Supplementary Discussion

Geometrical model of scFv binding to a single FL-pc-QD

To estimate the probability that several 4M5.3 scFv-Prp molecules diffuse around and bind to a single FL-pc-QD via multiple FL molecules, we use a simple geometrical model in which the QD is represented as a 12 nm diameter sphere (Fig. S6A) and the scFv is approximated by a truncated pyramid with a rectangular base with dimensions corresponding to the known crystallographic structure (Fig. S6B & C). We want to estimate the maximum packing of scFv molecules around the QD and the constraints this imposes on the scFv to cell membrane distance (see Fig. S6D).

The maximum packing density can be estimated using the solid angle occupied by a scFv in close contact with the QD. Since the “model” pyramid has a rectangular base ($w_1 \times w_2$), there are two planar angles α_1 and α_2 which are easily calculated by:

$$\tan \frac{\alpha_i}{2} = \frac{w_i}{2(R+h)} \quad (7)$$

With $R = 6$ nm, $h = 4.4$ nm, $w_1 = 3.6$ nm and $w_2 = 6.7$ nm, we obtain $\alpha_1 = 20^\circ$ and $\alpha_2 = 36^\circ$. The corresponding solid angle is given by:

$$\Omega = 4 \arcsin \left(\sin \frac{\alpha_1}{2} \sin \frac{\alpha_2}{2} \right) = 0.209 \text{ steradian} \quad (8)$$

Consequently, about $4\pi/\Omega = 60$ scFv molecules can be tightly packed around the QD.

Assuming tight packing of scFvs, we are interested in knowing how far away from the membrane each scFv needs to be extended to attain the next available binding spot on the

QD. As depicted on Fig. S6D, this is easily estimated from simple trigonometry. The minimum distance that the n^{th} nearest neighbor to the “lowest” scFv needs to extend, z_n , is given by:

$$z_n = (R + h)(1 - \cos n\alpha) \quad (9)$$

where α is either one of the two angles calculated before and depends on how the scFvs are packed (along their short or long edges). For α_1 (stacking along the long edge), we find that the next scFv needs to bind 0.6 nm higher, the following one ($n = 2$) 2.3 nm higher and 5 nm higher for $n = 3$. Along α_2 , the increase is even more rapid, since the next scFv needs to bind 2 nm higher and the following one 7.1 nm higher. Although crude estimates, these figures show that unless the scFv is free to extend significantly away from the membrane (> 2 nm), no binding can be expected except for a couple of scFvs stacked against the center one (there are 4 such positions available in our crude geometric model, but 2 correspond to binding sites that are 2 nm higher than the central binding site).

However, for this to happen, FL molecules need to be as tightly packed as our model assumes scFvs to be, that is, as 60 molecules disposed around a 12 nm diameter sphere would be. In our experiments, however, FL-pc-QDs are coated by at most 25 FL molecules, which can therefore not satisfy this requirement of tight packing. Therefore even the likelihood of a few tightly packed scFvs to bind the same QD is negligible.

Supplementary Figures and Movie Captions

Fig. S1: *S. cerevisiae* expressing clone 4M5.3 scFv stained with Alexa Fluor 647 anti-myc. Full length expression of the protein was checked by monitoring the presence of the C-terminal myc tag by direct immunofluorescence using Alexa-647 anti-myc antibody. Left: DIC image. Right: Galactose induced yeast stained with Alexa Fluor 647 anti-myc antibodies. Images were acquired on a TCS SP2 AOBS confocal microscope (Leica Microsystems, Exton, PA) with a 633 nm laser excitation and a 63 X oil-immersion objective (HCX PL APO, NA 1.40).

Fig. S2: Wide field imaging of *S. cerevisiae* strain expressing 4M5.3 ScFv displayed on the cell wall. Images from left to right: transmission, green fluorescence and red fluorescence. A: Induced cells labeled with 10 μ M FL-dextran show peripheral staining in the FL channel (green). B: Uninduced cells labeled with 10 μ M FL-dextran do not exhibit any fluorescence in either channel. C: Induced cells labeled with 10 nM FL-pc-QDs show peripheral staining in both the FL channel and the QD channel (red). Scale bar: 5 μ m.

Fig. S3: Representative FACS measurement of the dissociation constant K_D between 4M5.3 scFv displayed on yeast cells and FL-pc-QDs with different FL-p:K-p coverage (from top to bottom: 10: 90, 50 : 50, 100: 0) obtained with the QD signal. For each condition, a representative curve of the average fluorescence signal per cell at a given concentration of FL-pc-QD is shown. The average fitted value of the dissociation constant for this condition is indicated above each curve. Notice that the fitted K_D value obtained for the 10 % FL-pc-QD sample using the QD channel (top panel) is 3 orders of magnitude larger than the other values.

Fig. S4: Representative FACS measurements showing the percentage of cells with non-zero FL and QD fluorescence signals (from top to bottom: 10: 90, 50 : 50, 100: 0 FL-pc-QD). When possible, a simple binding model was fitted to the data. The corresponding mean dissociation constant $\langle K_D \rangle$ is indicated on the graph.

Fig. S5: Ensemble confocal imaging of N2a mouse neuroblastoma cells. Images from left to right: Differential interference contrast (DIC), green fluorescence and red fluorescence. Cells were labeled with 2 nM FL-pc-QD. A: Untransfected N2a cells show minimal non-specific labeling, B: Stably transfected N2a cell line expressing the scFv-PrP construct show intense surface labeling. Scale bar: 10 μm .

Fig. S6: Tight packing of truncated pyramids around a sphere. A: a QD is represented by a 12 nm diameter sphere; B, C: a 4M5.3 scFv molecule (to scale) is schematized by a truncated pyramid of height $h = 4.4$ nm and a rectangular base of size $w_1 \times w_2$ ($w_1 = 3.6$ nm, $w_2 = 6.7$ nm) as obtained from the crystal structure. D: Two dihedral angles α can be defined along the two axes of the truncated pyramid, allowing the calculation of the solid angle covered by a single scFv. The attachment sites of each successive layer of scFv (black dots) are raised above the membrane reference plane by increasing amounts (z_n) as one goes further away from the scFv closest to the surface (represented in the center).

Supplementary Movie 1: 3-D reconstruction of single-QD-decorated yeast cell was obtained from 24 XY dual-color images acquired by stage-scanning confocal microscopy separated by 0.5 μm in the Z direction. Each image covered $12 \times 12 \mu\text{m}^2$ with 100 nm/pixel and 5 ms integration/pixel. Excitation power at 488 nm: 3 μW , pinhole: 50 μm . The maximum intensity projection function of Metamorph (Molecular Devices,

Sunnyvale, CA) was used to generate projection images along different directions separated by 10°.

Supplementary References

1. Dabbousi, R. O.; Rodriguez-Viejo, J.; Mikulec, F. V.; Heine, J. R.; Mattoussi, H.; Ober, R.; Jensen, K. F.; Bawendi, M. G. *J. Phys. Chem. B* **1997**, 101, 9463-9475.
2. Pinaud, F.; King, D.; Moore, H.-P.; Weiss, S. *J. Am. Chem. Soc.* **2004**, 126, 6115-6123.
3. Iyer, G.; Pinaud, F.; Tsay, J.; Weiss, S. *Small* **2007**, 3, (5), 793-798.
4. Yu, W. W.; Qu, L. H.; Guo, W. Z.; Peng, X. G. *Chemistry of Materials* **2003**, 15, (14), 2854-2860.
5. Yu, W. W.; Qu, L.; Guo, W.; Peng, X. *Chem. Mater.* **2004**, 16, (3), 560.
6. Boder, E. T.; Midelfort, K. S.; Wittrup, K. D. *Proc. Nat. Acad. Sci. USA* **2000**, 97, 10701-10705.
7. Chao, G.; Lau, W. L.; Hackel, B. J.; Sazinsky, S. L.; Lippow, S. M.; Wittrup, K. D. *Nature Protocols* **2006**, 1, (2), 755-768.
8. Lacoste, T. D.; Michalet, X.; Pinaud, F.; Chemla, D. S.; Alivisatos, A. P.; Weiss, S. *Proceedings of the National Academy of Sciences USA* **2000**, 97, (17), 9461-9466.
9. Pinaud, F. F.; Michalet, X.; Iyer, G.; Margeat, E.; Moore, H. P.; Weiss, S. *submitted* **2008**.

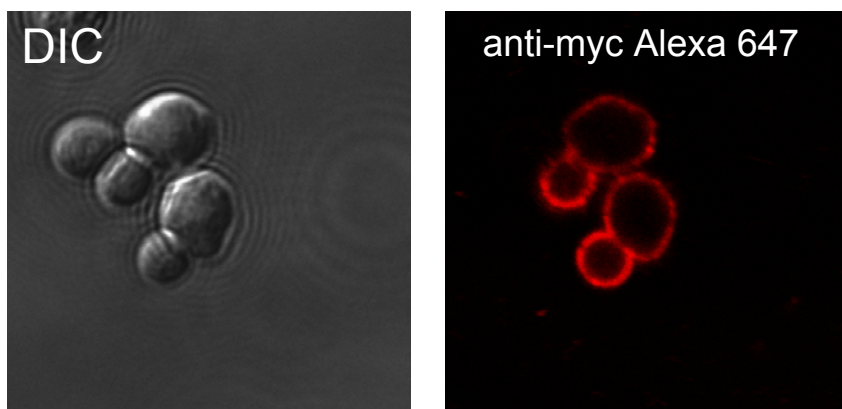


Fig. S1

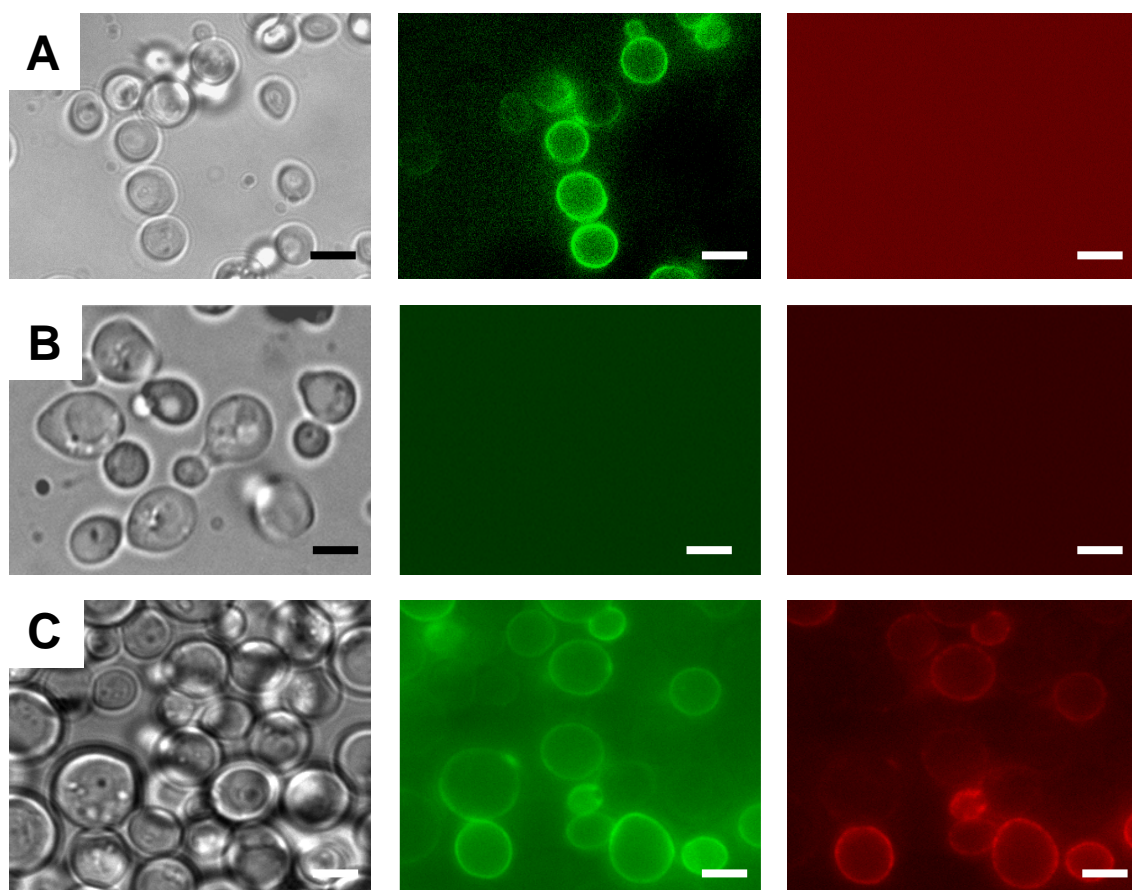
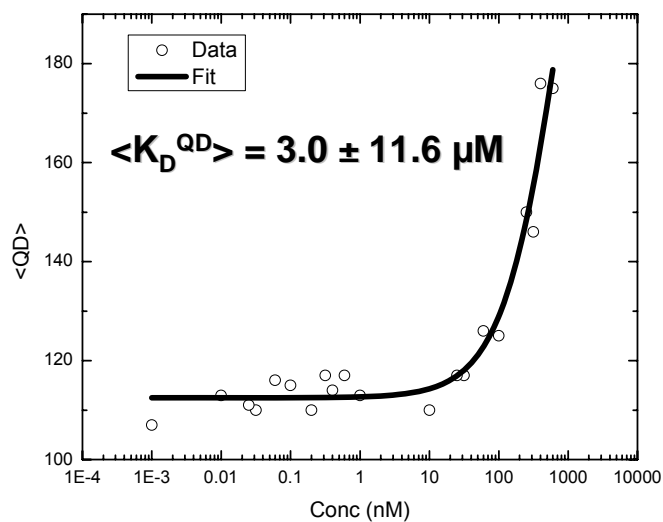
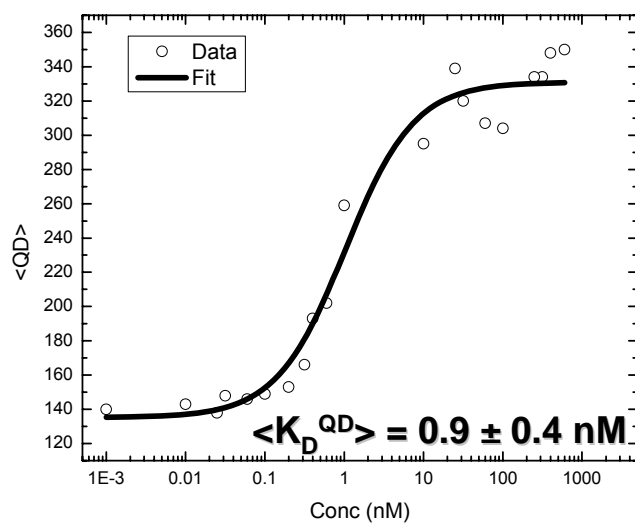


Fig. S2

10 % FL-pc-QD



50 % FL-pc-QD



100 % FL-pc-QD

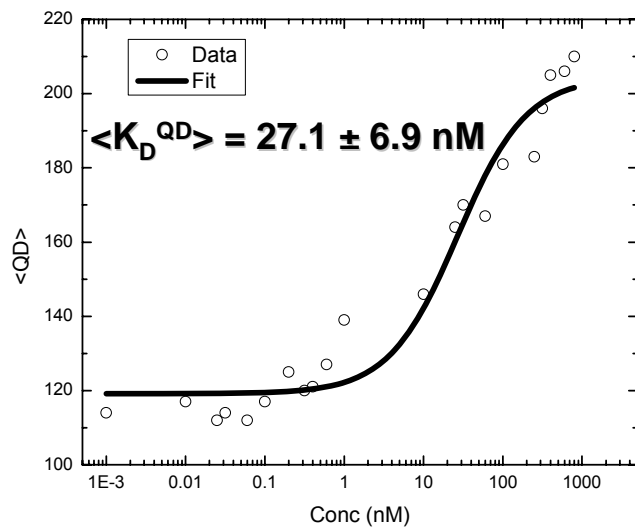
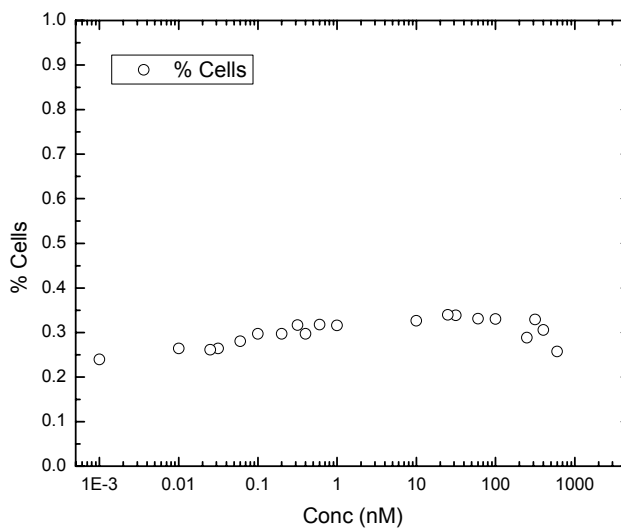
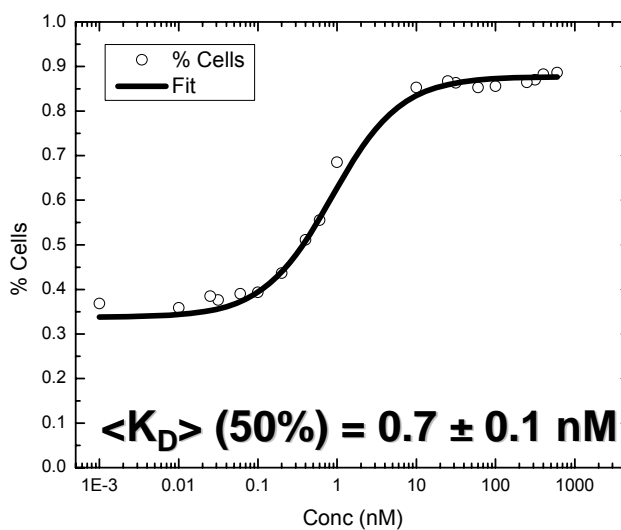


Fig. S3

10 % FL-pc-QD



50 % FL-pc-QD



100 % FL-pc-QD

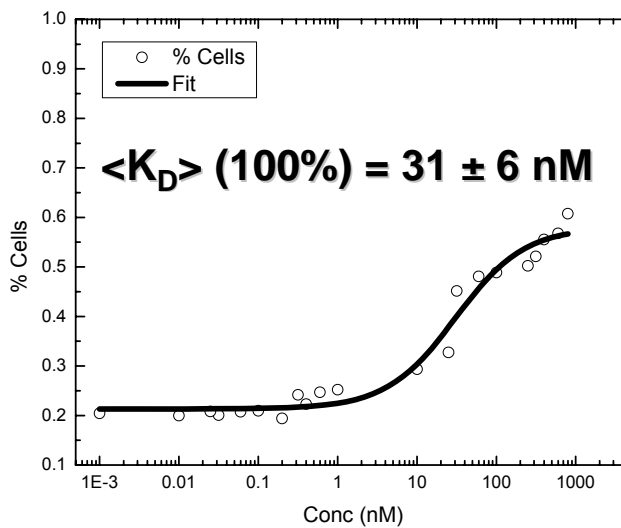


Fig. S4

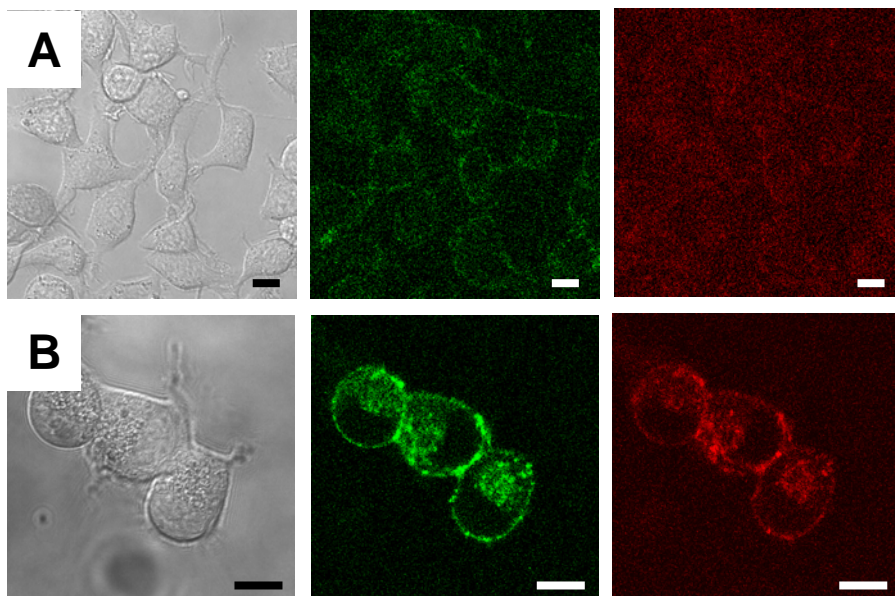
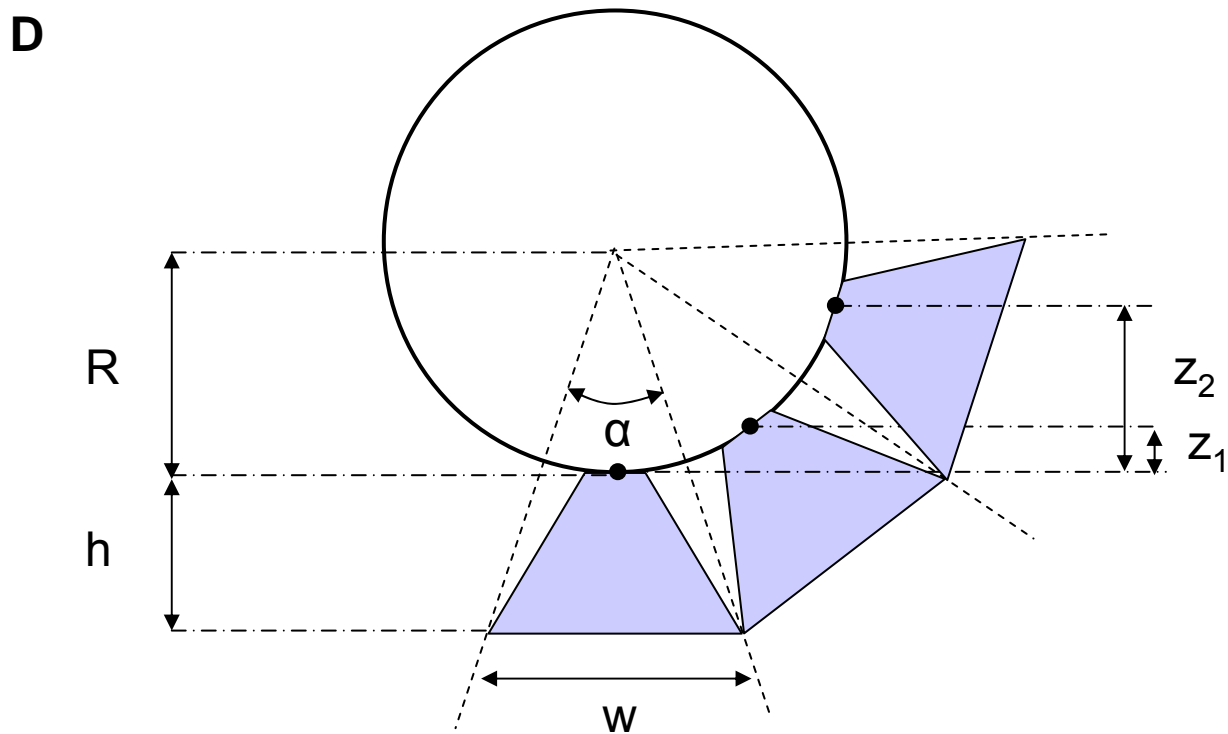
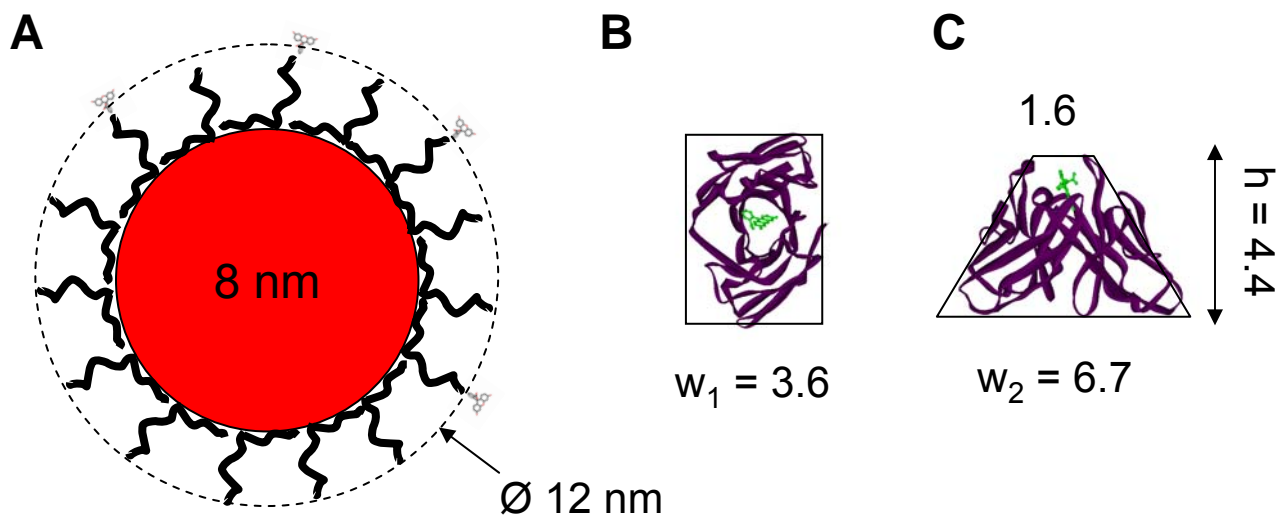


Fig. S5



upper leaflet (cell membrane)

Fig. S6